Translational Stroke Research (2019) 10:684–694
https://doi.org/10.1007/s12975-018-0685-0

ORIGINAL ARTICLE

The Role of Oxidative Stress in Microvascular Disturbances after Experimental Subarachnoid Hemorrhage

Toshio Fumoto[1] · Masato Naraoka[1] · Takeshi Katagai[1] · Yuchen Li[1] · Norihito Shimamura[1] · Hiroki Ohkuma[1]

Received: 12 September 2018 / Revised: 30 November 2018 / Accepted: 28 December 2018 / Published online: 9 January 2019

Abstract

Oxidative stress was shown to play a crucial role in the diverse pathogenesis of early brain injury (EBI) after subarachnoid hemorrhage (SAH). Microcirculatory dysfunction is thought to be an important and fundamental pathological change in EBI. However, other than blood-brain barrier (BBB) disruption, the influence of oxidative stress on microvessels remains to be elucidated. The aim of this study was to investigate the role of oxidative stress on microcirculatory integrity in EBI. SAH was induced in male Sprague-Dawley rats using an endovascular perforation technique. A free radical scavenger, edaravone, was administered prophylactically by intraperitoneal injection. SAH grade, neurological score, brain water content, and BBB permeability were measured at 24 h after SAH induction. In addition, cortical samples taken at 24 h after SAH were analyzed to explore oxidative stress, microvascular mural cell apoptosis, microspasm, and microthrombosis. Edaravone treatment significantly ameliorated neurological deficits, brain edema, and BBB disruption. In addition, oxidative stress-induced modifications and subsequent apoptosis of microvascular endothelial cells and pericytes increased after SAH induction, while the administration of edaravone suppressed this. Consistent with apoptotic cell inhibition, microthromboses were also inhibited by edaravone administration. Oxidative stress plays a pivotal role in the induction of multiple pathological changes in microvessels in EBI. Antioxidants are potential candidates for the treatment of microvascular disturbances after SAH.

Keywords Early brain injury · Subarachnoid hemorrhage · Oxidative stress · Microvessel

Introduction

Subarachnoid hemorrhage (SAH), which predominantly occurs secondarily to aneurysmal rupture, remains one of the most severe neurological diseases, with high mortality and morbidity in spite of advances in therapeutic and diagnostic techniques. In addition to its severity, the fact that it mainly afflicts relatively young patients causes an enormous socioeconomic burden despite being a rare subtype of stroke. Therefore, increased attention has been given to understanding the molecular mechanisms responsible for SAH [1].

Cerebral vasospasm (CVS), a major sequelae of SAH, had been considered an important cause of delayed ischemic neurological deficits and poor outcome and thus previous research focused predominantly on CVS [2]. However, since the clinical trials with clazosentan [3, 4], other pathological changes have gained increasing attention [5–10].

The term "early brain injury" (EBI) was coined to describe extensive brain injuries that occur in the period between initial bleeding and the onset of CVS. Diverse pathological changes that include blood-brain barrier (BBB) disruption, brain edema, cerebral ischemia, and neuronal cell death are involved in EBI [6, 7]. Microcirculatory disturbance is a critical pathological change in EBI, since it influences various other pathological EBI changes. Vasoconstriction and thrombosis in microvessels cause cerebral ischemia and neuronal cell death. Brain edema occurs as a consequence of BBB disruption in capillaries. In addition, microcirculatory disturbance is hypothesized to be involved in the development of delayed cerebral ischemia and poor outcome [11].

Oxidative stress plays a crucial role in the induction of diverse pathological changes in EBI. Oxyhemoglobin, a

Electronic supplementary material The online version of this article (https://doi.org/10.1007/s12975-018-0685-0) contains supplementary material, which is available to authorized users.

✉ Hiroki Ohkuma
ohkuma@hirosaki-u.ac.jp

[1] Department of Neurosurgery, Hirosaki University Graduate School of Medicine, 5 Zaifucho, Hirosaki, Aomori 036-8562, Japan

component of blood clots distributed in the subarachnoid cavity, generates reactive oxygen species (ROS) by itself. Mitochondrial and enzymatic generation of ROS are also enhanced, whereas endogenous antioxidant protection systems are suppressed immediately after SAH induction. Thus, oxidative stress is dramatically elevated and influences various signaling pathways that lead to a variety of pathological changes in EBI [12]. In fact, pharmacological and genetic suppression of oxidative stress have been shown to alleviate diverse components of EBI, whereas enhancement of oxidative stress aggravates them [13–17]. However, it has not been clarified whether oxidative stress plays a causative role in microcirculatory disturbances other than BBB disruption. The aim of this study was to investigate the influences of oxidative stress on microcirculation after SAH by examining the changes induced by the administration of an antioxidant.

Material and Methods

All experimental procedures were performed in accordance with the Guidelines for Animal Experimentation of Hirosaki University, and the experimental protocols were reviewed and approved by the Animal Research Committee of Hirosaki University.

Animals

Adult male Sprague-Dawley rats (10–13 weeks old, 400–450 g) from CLEA Japan, Inc. (Japan) were used in this study. The animals were maintained under standard laboratory conditions (25 ± 2 °C, 12 h light/dark cycle) and allowed free access to water and standard pellet chow.

Experimental Design

The rats were randomly divided into three groups. The edaravone group was treated with edaravone (1.5 mg/1 kg, intraperitoneally) at 30 min before SAH induction and subjected to SAH. The SAH group was injected with the same volume of saline and subjected to SAH. The Sham group was subjected to the same procedure as the SAH group without endovascular perforation.

SAH Model

The modified endovascular perforation technique was used to establish the SAH model in this study with a slight modification [18]. The rats were anesthetized using a combination anesthetic (medetomidine = 0.3 mg/kg, midazolam = 4 mg/kg, butorphanol = 5 mg/kg). A perfluoroalkoxy alkane (PFA) micro tube (ID = 0.2 mm, OD = 0.4 mm) and a tungsten wire (diameter = 0.1 mm) were used in this study.

SAH Grades

The severity of the SAH was evaluated using a previously published grading scale [19].

Neurological Evaluation

Neurological deficits were evaluated at 24 h after SAH induction using a previously published scoring system [20].

Brain Water Content

Rats were decapitated under deep anesthesia at 24 h after SAH induction and their brains were extracted and divided into four segments: right hemisphere, left hemisphere, cerebellum, and brain stem. Each part of the brain was weighed immediately to determine the wet weight. The samples were then dried at 105 °C for 48 h to obtain dry weights. Brain water contents were calculated as follows: [(wet weight − dry weight)/wet weight] × 100%.

Evans Blue Extravasation

Under deep anesthesia, Evans blue dye (2% in saline, 5 ml/kg) was injected into the right femoral vein at 24 h after SAH induction and allowed to circulate for 60 min. After the addition of anesthetic agents, rats were euthanized by transcardial perfusion with PBS. The brains were removed and divided into the same four parts as for brain water content. Brain samples were weighed and cryopreserved. After homogenization in an equal volume of 50% TCA, samples were incubated at 4 °C overnight and centrifuged at 15,000*g* for 30 min. The supernatant was measured for absorbance at 620 nm by spectrophotometry (Thermo Scientific, USA).

Western Blotting

Western blotting was performed as previously described [21]. Briefly, rats were transcardially perfused with PBS under deep anesthesia and their brains were collected at 24 h after SAH induction. Proteins of the ipsilateral left parietal cortex were extracted by homogenization in RIPA buffer containing protease inhibitors (Santa Cruz Biotechnology, USA) and centrifuged. Protein concentrations were determined using a BCA protein assay (Bio-Rad, USA). Equal amounts of protein were subjected to 10% SDS-PAGE and transferred to PVDF membranes. After blocking, the membranes were incubated with primary antibody and then with peroxidase-conjugated secondary antibody. Bands were visualized using ECL substrates (Amersham ECL Select Western Blotting Detection Reagents (GE Healthcare, UK) or SuperSignal West Femto Substrate (Pierce, USA)) and ChemiDoc XRS Plus (Bio-Rad, USA). Bands were quantified by Image Lab software (Bio-Rad,

USA). The antibodies used in this study are listed in Supplemental Table 1.

Dot Blot

Protein samples were prepared by the same procedure as of western blotting. Equal amounts of protein were spotted onto nitrocellulose membrane. After incubation for 1 h at room temperature, the membranes were blocked and incubated with primary antibody and then with secondary antibody. Dots were visualized and quantified by the same methods as of western blotting.

TUNEL and Immunohistological Staining

The rats were perfused transcardially with PBS and 4% paraformaldehyde under deep anesthesia at 24 h after SAH induction. Brains were removed, fixed overnight using the same fixative and cryoprotected by immersion using gradient sucrose (10%, 20%, 30%) dissolved in PBS for 1 day each. The specimen was frozen in OCT compound (Sakura Finetek, Japan) and cut into 6-μm-thick coronal sections using a cryostat (Zeiss, Germany).

Immunohistochemical analysis of endogenous IgG, nitrotyrosine, and 8-hydroxyguanosine was performed as previously described [22]. Briefly, sections were blocked with normal goat serum and treated with BLOXALL (Vector Laboratories, USA) and an Avidin/Biotin Blocking Kit (Vector Laboratories, USA). The sections were incubated with antibodies, Vectastatin Elite ABC Kit (Vector Laboratories, USA), and ImmPACT DAB (Vector Laboratories, USA). After counterstaining with hematoxylin, slides were observed using a light microscope (Olympus, Japan).

For TUNEL staining, sections were incubated with primary antibody and then with Alexa Fluor-conjugated secondary antibody. TUNEL reaction was performed using the In Situ Cell Death Detection Kit, Fluorescein (Roche). Slides were observed using a fluorescent microscope (KEYENCE, Japan). TUNEL-positive cells were counted in the high-resolution TUNEL staining images using DAPI as a reference. For double immunofluorescence staining of collagen IV and matrix metalloproteinase-9 (MMP-9), or collagen IV and fibrin, the same procedure was conducted as for TUNEL staining but without the TUNEL reaction.

Basement membrane external diameter and basement membrane thickness were measured on high-resolution images of collagen IV immunofluorescence staining. Forty circular sections of microvessels were measured and the mean was defined as the microvascular diameter and wall thickness for each animal. Fibrin-positive microvessels were counted in the high-resolution images of collagen IV and fibrin double staining. The percentage of fibrin positive microvessels was determined using at least 290 collagen IV positive microvessels for each animal. All immunohistological analyses were performed on the parietal cortex of the ipsilateral, left side.

Gelatin Zymography

Proteins were extracted from the ipsilateral left parietal cortex and separated using gels containing 10% acrylamide and 0.1% gelatin. The gels were visualized using a gelatin-zymography kit (Cosmo Bio, Japan) following the manufacturer's instructions and high-resolution images were taken.

Statistical Analysis

All statistical analyses were performed using JMP13 software. Mortality was evaluated by Fisher's exact test. The other measurements were initially analyzed by Shapiro-Wilk test. SAH grade, Neurological scores, and TUNEL staining were analyzed using Kruskal-Wallis tests followed by Steel-Dwass test for multiple comparisons. All the other data were analyzed by one-way analysis of variance (ANOVA) followed by Tukey-Kramer test for post hoc comparisons. The data are presented as means and SD. Statistical significance was defined as $P < 0.05$.

Results

Administration of Edaravone Improved Neurological Functions

We first confirmed the influence of edaravone on the extent of bleeding itself. As shown in Fig. 1a, edaravone treatment did not alter the SAH grade. We next examined the effects of edaravone treatment on neurological outcome. No rats in the sham group died in the course of our experiments. At 24 h after SAH induction, the mortality rate of the SAH group and the edaravone group was 25.0% and 21.7%, respectively. The mortality rate of the edaravone group was slightly lower than that of the SAH group, but there was no significant difference between them. By contrast, the neurological score of the edaravone group was significantly higher than of the SAH group at the same point in time (Fig. 1b).

Edaravone Suppressed Oxidative Stress Especially in Microvessels

We next examined the effects of edravone on oxidative stress-mediated modification of microvessels during EBI by immunostaining. Nitrotyrosine and 8-hydroxydeoxyguanosine (8-OHdG) are specific markers of oxidative stress in protein and DNA, respectively. In the sham group, only slight staining of nitrotyrosine was detected. In contrast, clear staining was

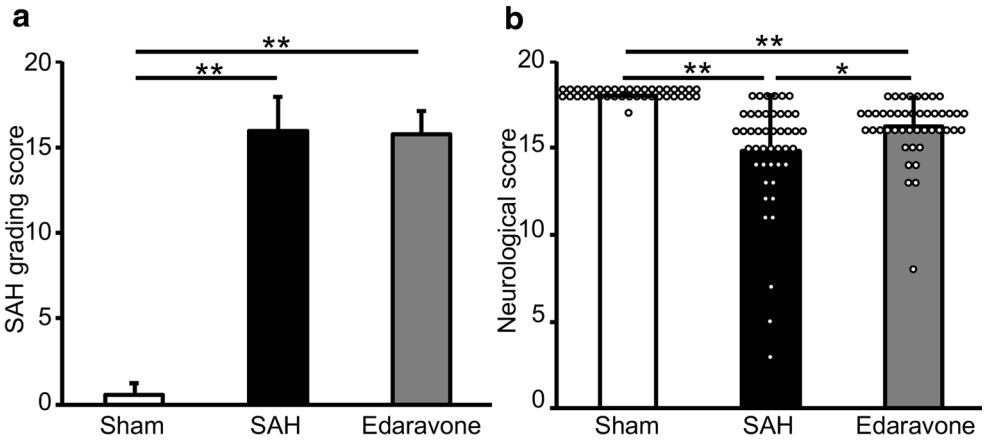

Fig. 1 Effect of edaravone on subarachnoid hemorrhage (SAH) severity and neurological defects. **a** SAH grading scores were evaluated at 24 h after SAH induction. $n = 12$ for each group. **b** Neurological scores were assessed at 24 h after surgery. $n = 39$ for the Sham group, $n = 45$ for the SAH group and the edaravone group. All data are expressed as mean and SD. *$P < 0.05$, **$P < 0.01$

seen both in vascular cells and perivascular cells of the SAH group. Edaravone treatment clearly suppressed this staining, especially in vascular cells (Fig. 2a, upper). 8-OHdG immunostaining showed the same trends (Fig. 2a, bottom). Dot blot confirmed these effects of edaravone on oxidative stress (Fig. 2b, c).

Edaravone Decreased BBB Permeability and Suppressed Brain Edema

The blood-brain barrier, a unique feature of cerebral microvessels, is known to be disrupted and to induce brain edema after SAH. We determined brain water contents at 24 h after SAH induction. The brain water contents of the SAH group were higher than for the sham group in all areas examined. The brain stem was the only site that did not show a statistical difference. Edaravone treatment suppressed these increases, especially in the left and right cerebral hemispheres (Fig. 3a).

To investigate BBB permeability, we injected Evans blue dyes at 24 h after SAH induction and measured extravasated dye 1 h later. Evans blue extravasations were significantly increased in all areas of the SAH group compared to the sham group. Edaravone treatment almost completely suppressed these increases in the ipsilateral, left hemisphere (Fig. 3b). To investigate BBB permeability using endogenous substances, we next stained IgG at 24 h after SAH. In the sham group, no extravasated IgG was detected. In contrast, clear IgG staining was seen especially in the perivascular region of the SAH group. Edaravone treatment suppressed these extravasations of

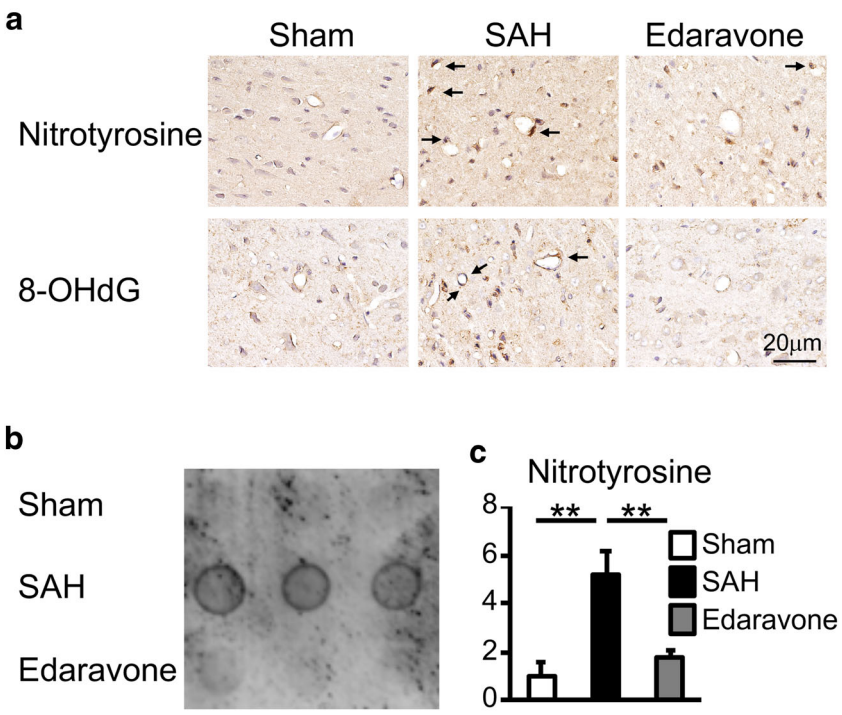

Fig. 2 Effect of edaravone on oxidative stress. **a** Representative immunostaining pictures of nitrotyrosine and 8-hydroxydeoxyguanosine (8-OHdG) in the cerebral cortex at 24 h after SAH induction. Arrows indicate strong staining of oxidative stress markers in vascular cells. **b** Representative dot blots of nitrotyrosine at 24 h after SAH induction. **c** Quantification of dot blots. $n = 3$ for each group. Data are expressed as mean and SD. **$P < 0.01$

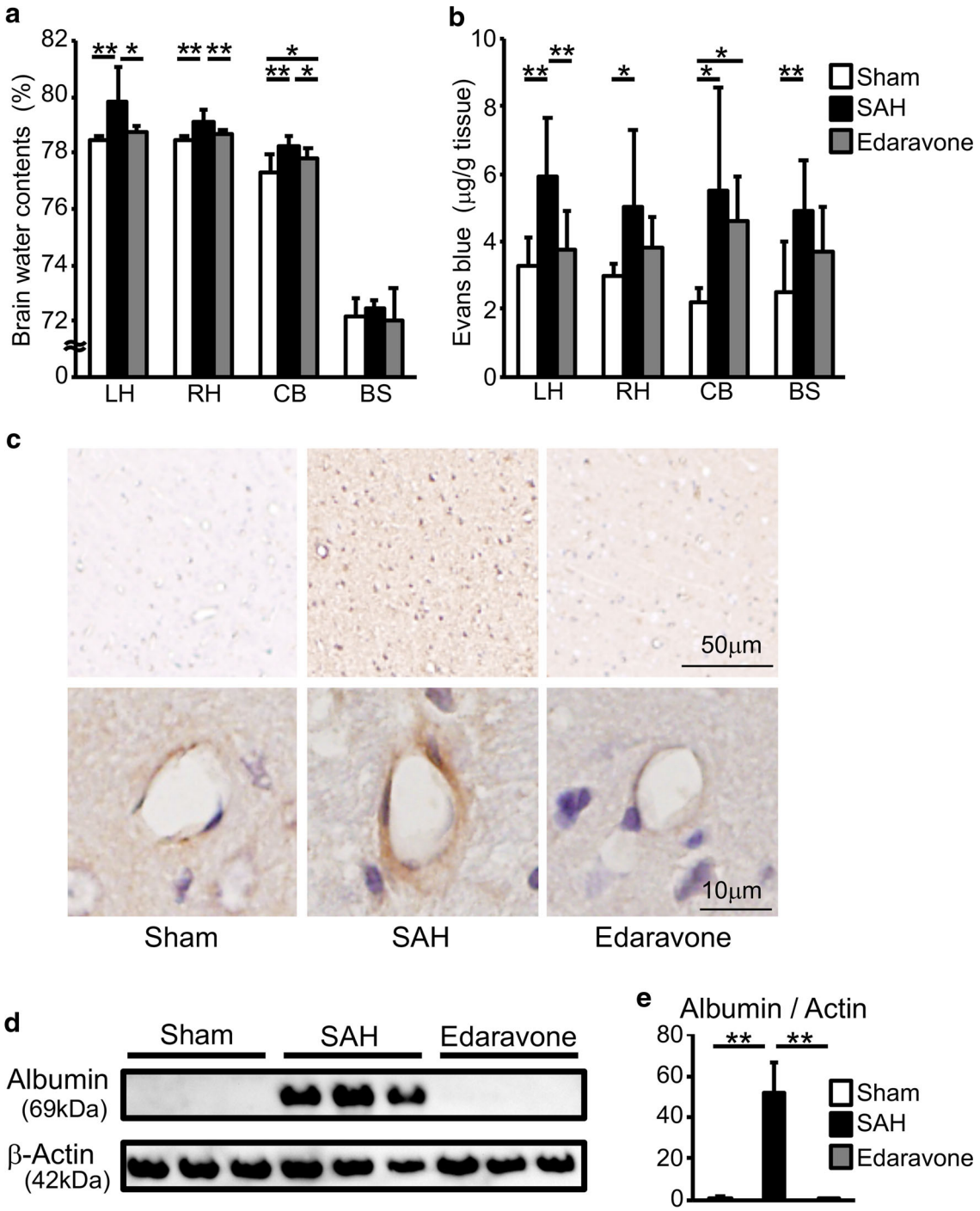

Fig. 3 Effect of edaravone on brain edema and blood-brain barrier (BBB) permeability. **a** Brain water contents of the left hemisphere (LH), right hemisphere (RH), cerebellum (CB), and brainstem (BS) were evaluated at 24 h after SAH induction. **b** Evans blue dye extravasation was assessed at 24 h after SAH. $n = 9$ for the Sham group, $n = 12$ for the SAH group, and the edaravone group. Data are expressed as mean and SD. *$P < 0.05$, **$P < 0.01$. **c** Representative immunostaining pictures of endogenous IgG of the cerebral cortex at 24 h after surgery. **d** Representative western blots of extravasated albumin at 24 h after SAH induction. β-actin was used as a loading control. **e** Quantification of albumin expression. $n = 3$ for each group. Data are expressed as mean and SD. ** $P < 0.01$

endogenous IgG (Fig. 3c). To investigate these endogenous extravasation quantitatively, we examined the expression of albumin in perfused brain tissues. As shown in Fig. 4d, e, albumin was extravasated after SAH and edaravone treatment almost completely suppressed them.

Edaravone Inhibited MMP-9 and Preserved Tight Junction Proteins

To gain some mechanistic insight into these protective effects of edaravone, we examined the expressions of tight junction

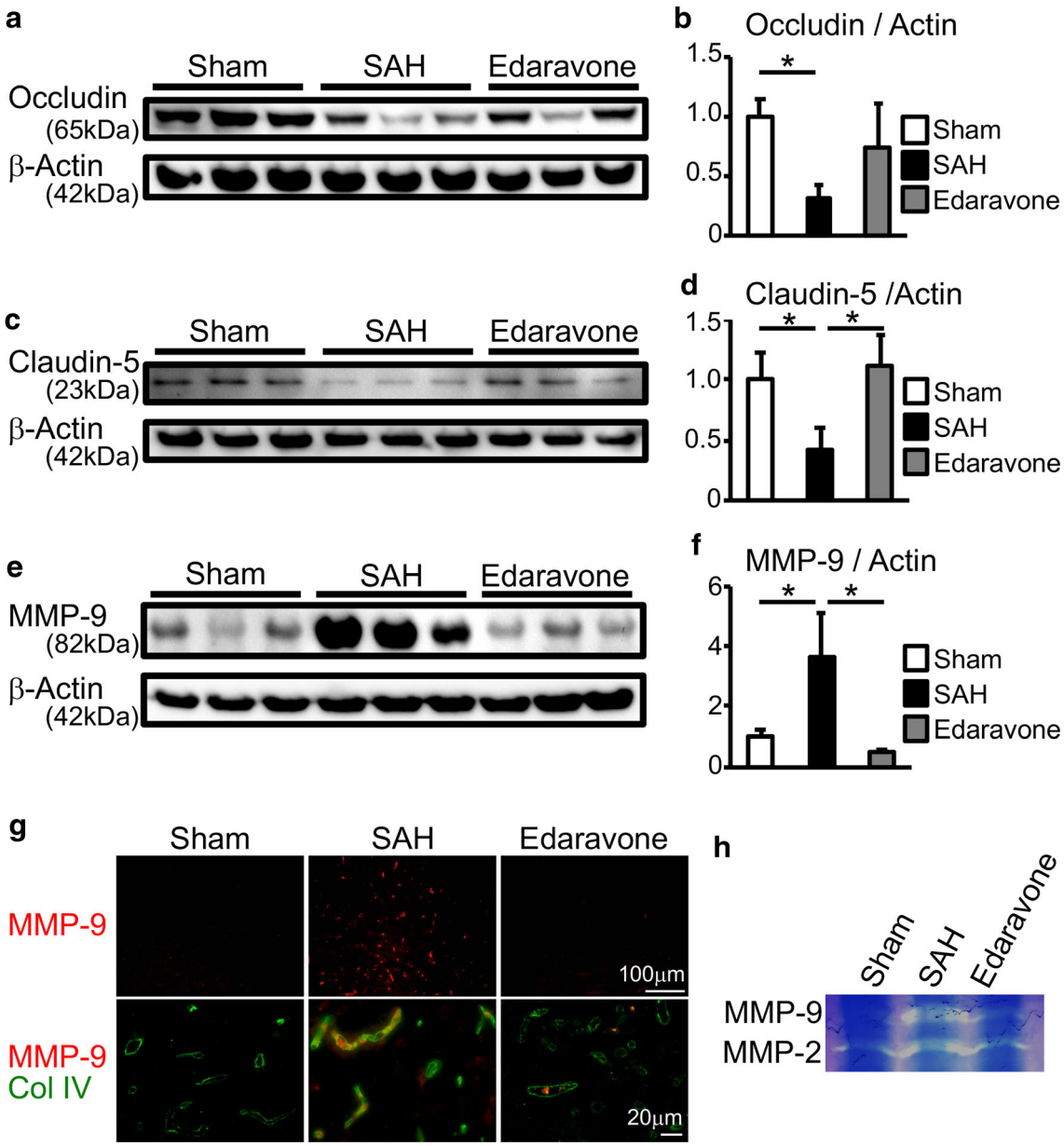

Fig. 4 Effect of edaravone on tight junction proteins and matrix metalloproteinase-9 (MMP-9). Representative western blots of occludin (**a**), claudin-5 (**c**), and MMP-9 (**e**) at 24 h after SAH induction. β-actin was used as a loading control. Quantification of occluding (**b**), claudin-5 (**d**), and MMP-9 (**f**) expression. $n = 3$ for each group. Data are expressed as mean and SD. $^{*}P < 0.05$, $^{**}P < 0.01$. **g** Representative immunofluorescence pictures of MMP-9 and collagen IV (Col IV) in the cerebral cortex. **h** Representative gelatin zymography showing activities of MMP-9

proteins at 24 h after SAH induction. The expressions of occludin and claudin-5 decreased in the SAH group compared to the sham group. Edaravone treatment prevented these reductions (Fig. 4a–d). Next, we examined the expression and activity of MMP9. Western blotting analysis showed that active forms of MMP-9 were induced along with SAH and these inductions were apparently suppressed by edaravone treatment (Fig. 4e, f). Immunostaining analysis confirmed these inductions and suppression (Fig. 4g, upper). In addition, immunostaining analysis showed these inductions occurred around microvessels in the cerebral cortex (Fig. 4g, *bottom*). Consistent with these results, the activities of MMP-9 were induced along with SAH induction and suppressed by edaravone (Fig. 4h).

Edaravone Protected Microvessel Integrity

In addition to tight junctions, endothelial cells, per se, play a critical role in the blood-brain barrier. We performed TUNEL staining at 24 h after SAH induction.

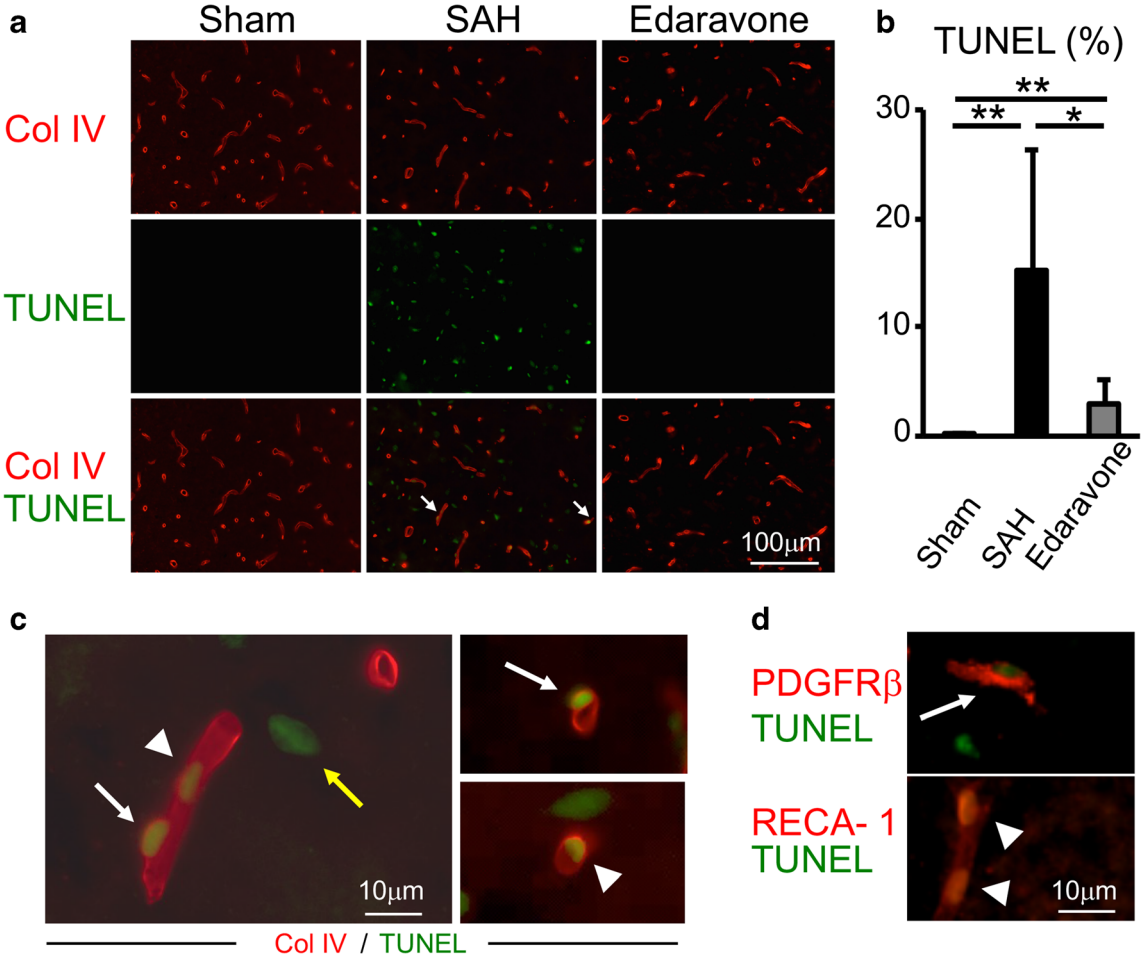

Fig. 5 Effect of edaravone on vascular cell integrity. **a** Representative pictures of collagen IV (Col IV) immunostaining and terminal deoxynucleotidyl transferase-mediated dUTP nick-end labeling (TUNEL) staining. Note that microvascular narrowings near TUNEL positive cells were seen in the SAH group (arrow). **b** Quantification of TUNEL positive cells. Data are expressed as percentages of total cells counted by DAPI staining. $n = 9$ for each group. Values are mean and SD. $^{*}P < 0.05$, $^{**}P < 0.01$. **c** High magnification image of Col IV and TUNEL double staining of the SAH group. **d** High magnification image of PDGFRβ and TUNEL double staining or RECA-1 and TUNEL double staining of the SAH group. Note that TUNEL positive cells were seen at the outside of microvessels (yellow arrow), as were TUNEL positive pericytes surrounded by basal lamina on the outside of endothelium (arrow) and TUNEL positive endothelial cells at the inside of basal lamina (arrow head)

As shown in Fig. 5a, b, SAH induced TUNEL positive apoptotic cells and edaravone treatment suppressed these inductions. TUNEL and collagen IV double staining showed three types of TUNEL positive cells in the SAH group; TUNEL positive cells outside of microvessels, TUNEL positive cells inside of collagen IV positive vascular wall and TUNEL positive cells surrounded by collagen IV staining in the vascular wall (Fig. 5c). As shown in Fig. 5d, these TUNEL positive mural cells included PDGFRβ positive cells and RECA-1 positive cells.

Edaravone Suppressed Microthrombosis

We next performed collagen IV and fibrin immunostaining at 24 h after SAH induction in order to evaluate the effect of altered vascular cell integrity. Very few fibrin-positive microvessels were seen in the sham group. SAH enhanced fibrin deposition in the microvessels and a substantial portion of microvessels were completely occluded. Edaravone treatment suppressed these microthrombi formations (Fig. 6a). Quantitative analyses confirmed that edaravone significantly suppressed microthrombosis (Fig. 6b). On the other hand, vascular diameter and basement membrane thicknesses were reduced with SAH and these reductions were partially inhibited by edaravone treatment. However, these changes were not statistically significant (Fig. 6c, d).

Discussion

Microcirculatory disturbances have been investigated as important pathological processes of EBI, but, except for the

BBB, the influences of oxidative stress on microcirculation are poorly understood. Therefore, we studied the changes in microvessels after SAH and the roles of oxidative stress on them.

One of the important functions of microvessels is creating the BBB. Tight junctions, the main factors constituting the BBB, have been shown to be disrupted and to induce brain edema after SAH. As one of its mechanisms, it has also been shown that MMP-9 is upregulated and degrades tight junction proteins in EBI [23]. In this study, we demonstrated that edaravone treatment prevents the expression and activation of MMP-9 and the subsequent degradation of tight junction proteins: claudin-5 and occludin. These results are consistent with previous reports using other antioxidants during EBI [24, 25]. We could not clarify the mechanism by which edaravone affects MMP-9 expression in this study. However, some known regulators of MMP-9 such as IL-1β, IL-6, TNF-α, and NF-κB [26–30], which are suppressed by other antioxidants in EBI [25, 31, 32] and by edaravone in other types of brain injury [33–35], may mediate the action of edaravone in

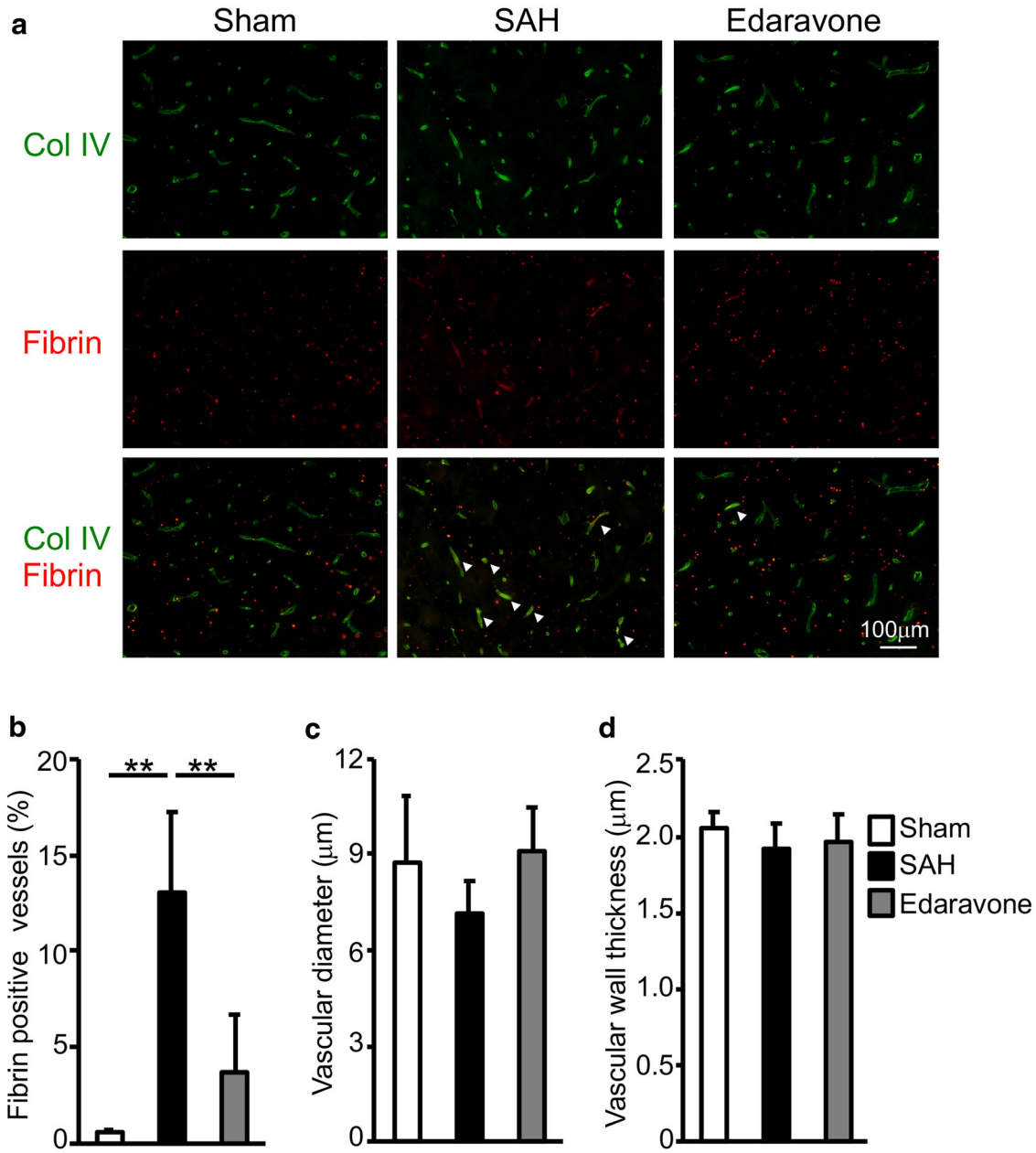

Fig. 6 Effect of edaravone on microvessel integrity. **a** Representative immunostaining pictures of collagen IV (Col IV) and fibrin in the cerebral cortex at 24 h after SAH induction. The percentage of fibrin positive microvessels (**b**), outer diameter of basement membrane (**c**), and basement membrane thickness (**d**) were evaluated. $n = 12$ for each group. Data are expressed as mean and SD. $^{**}P < 0.01$.

EBI. A recent study demonstrated that miR-21, which regulates MMP-9 expression and is inhibited by antioxidants, increases in SAH patients with delayed cerebral ischemia [36–38]. Therefore, epigenetic regulation may also contribute to these actions of edaravone.

In addition to tight junctions, vascular endothelial cells, per se, are also important constituents of BBB that limit transcellular transport [39]. Their barrier function may be disturbed, since endothelial cells that were RECA-1 positive and existed inside collagen IV positive basal lamina went into apoptosis after SAH in the present study. Edaravone treatment suppressed the induction of apoptosis, which indicates edaravone can preserve BBB integrity by not only maintaining tight junctions but also endothelial cell barrier function. These preventive effects of edaravone indicate that endothelial apoptosis in EBI can be mediated by oxidative stress.

Microspasm has been pointed to as another cause of microcirculatory disturbance in EBI [40]. The heterogeneous luminal narrowing of pial and parenchymal arterioles, which show a pearl-string-like appearance, have been demonstrated both in experimental and clinical studies [41–44]. It is not clear whether capillaries and venules could also constrict after SAH, since they lack smooth muscle cells [41, 45]. A recent study suggested that microspasm is mediated by a mechanism different from that of vasospasm in large vessels [46]. In the present study, we found narrowing of microvessels near their apoptotic mural cells after SAH. These apoptotic cells are considered as pericytes because of their locational characteristic and their PDGFRβ expression. Recent growing evidence from experimental studies indicates that changes in capillary diameter mediated by pericytes play a crucial role in the regulation of blood flow in various tissues including brain parenchyma [47–50]. Capillary constriction mediated by pericytes caused segmental luminal narrowing [48], and this constriction was followed by pericyte death [49]. Although we could find no statistical significance, even a subtle reduction in microvascular diameter after SAH can influence cerebral blood flow under the condition of low perfusion pressure. Because oxidative stress has been shown to play an important role in capillary constriction [50], slight amelioration of microvascular diameter, as seen in the edaravone treatment group, may be attributable to the suppression of oxidative stress. In addition to microvascular mural cells, we found here that edaravone suppressed apoptosis of non-vascular cells. These cells can also include neurons, because some other antioxidants were shown to suppress neural cell apoptosis in EBI [51, 52].

Microthrombosis is another important component of the microcirculatory disturbance in EBI [40, 53]. Experimental and clinical investigations have demonstrated microthrombi formation in brain parenchymal microvessels after SAH [54, 55]. Microthrombi in pial arterioles also appeared immediately after SAH using an in vivo imaging technique [41]. These microthromboses were shown to be inhibited by a fibrinolytic agent or thrombus formation inhibitor [56–58]. It was also demonstrated that peroxynitrite produced by eNOS uncoupling at large cerebral arteries leads to microthrombi at distal sites, and these microthromboses are inhibited by eNOS KO and simvastatin treatment [59–61]. Therefore, "hypercoagulability," one component of Virchow's triad, is considered to play an important role in microthrombus formation after SAH. In the present study, we demonstrated that fibrin deposition on microvessels is increased remarkably after SAH induction and edaravone treatment significantly suppresses this microthrombus formation. In addition, these changes correlated well with endothelial cell apoptosis and microvascular narrowing. Therefore, "endothelial damage" and "stasis of blood flow," the other components of Virchow's triad, may also contribute to microthrombus formation in EBI. Also, significant suppression of microthrombus formation achieved by edaravone administration might be due to the protective effects on endothelial cells and pericytes against oxidative stress.

There are several limitations in the present study. First, we could not clarify whether these effects of edaravone are the direct consequence of its antioxidative property or not. It has been reported that inflammation plays a crucial role in EBI and anti-inflammatory effects of edravone. Further studies using the other antioxidants are needed in the future. In addition, we could not characterize microspasm quantitatively in this study. Further studies, e.g., using real-time, in vivo imaging techniques at earlier points in time, are needed in the future. Moreover, we injected edaravone prophylactically in order to address the overall effects of edaravone treatment on EBI in this study. The dosage sensitivity and optimal therapeutic window remain to be elucidated.

In conclusion, we demonstrated that edaravone attenuates brain edema and BBB disruption by preventing degradation of tight junction proteins, as has been reported for other antioxidants. Furthermore, we also showed in this study that an antioxidant preserves microvascular mural cells from apoptosis and prevents microthrombosis after SAH, which had not yet been clarified. These data indicate that oxidative stress plays a pivotal role in the induction of multiple pathological changes in microvessels in EBI. Although further studies are need, our finding suggests that antioxidants are potential candidates for the treatment of EBI after SAH.

Acknowledgements The authors thank Mark Inglin (University of Basel) for his editorial assistance.

Funding This study was supported partially by JSPS KAKENHI Grant Number JP16K19993 (to MN).

Compliance with Ethical Standards

Conflict of Interest The authors declare that no conflict of interest exists.

Ethical Approval All applicable international, national, and/or institutional guidelines for the care and use of animals were followed.

Publisher's Note Springer Nature remains neutral with regard to jurisdictional claims in published maps and institutional affiliations.

References

1. Macdonald RL, Schweizer TA. Spontaneous subarachnoid haemorrhage. Lancet. 2017;389(10069):655–66.
2. Macdonald RL. Origins of the concept of vasospasm. Stroke. 2016;47(1):e11–5.
3. Macdonald RL, Kassell NF, Mayer S, Ruefenacht D, Schmiedek P, Weidauer S, et al. Clazosentan to overcome neurological ischemia and infarction occurring after subarachnoid hemorrhage (conscious-1): randomized, double-blind, placebo-controlled phase 2 dose-finding trial. Stroke. 2008;39(11):3015–21.
4. Macdonald RL, Higashida RT, Keller E, Mayer SA, Molyneux A, Raabe A, et al. Clazosentan, an endothelin receptor antagonist, in patients with aneurysmal subarachnoid haemorrhage undergoing surgical clipping: a randomised, double-blind, placebo-controlled phase 3 trial (conscious-2). Lancet Neurol. 2011;10(7):618–25.
5. Sehba FA, Pluta RM, Zhang JH. Metamorphosis of subarachnoid hemorrhage research: from delayed vasospasm to early brain injury. Mol Neurobiol. 2011;43(1):27–40.
6. Sehba FA, Hou J, Pluta RM, Zhang JH. The importance of early brain injury after subarachnoid hemorrhage. Prog Neurobiol. 2012;97(1):14–37.
7. Fujii M, Yan J, Rolland WB, Soejima Y, Caner B, Zhang JH. Early brain injury, an evolving frontier in subarachnoid hemorrhage research. Transl Stroke Res. 2013;4(4):432–46.
8. Neulen A, Meyer S, Kramer A, Pantel T, Kosterhon M, Kunzelmann S, et al. Large vessel vasospasm is not associated with cerebral cortical hypoperfusion in a murine model of subarachnoid hemorrhage. Transl Stroke Res. 2018. https://doi.org/10.1007/s12975-018-0647-6.
9. Conzen C, Albanna W, Weiss M, Kürten D, Vilser W, Kotliar K, et al. Vasoconstriction and impairment of neurovascular coupling after subarachnoid hemorrhage: a descriptive analysis of retinal changes. Transl Stroke Res. 2018;9(3):284–93.
10. Suzuki H, Shiba M, Nakatsuka Y, Nakano F, Nishikawa H. Higher cerebrospinal fluid pH may contribute to the development of delayed cerebral ischemia after aneurysmal subarachnoid hemorrhage. Transl Stroke Res. 2017;8(2):165–73.
11. Terpolilli NA, Brem C, Bühler D, Plesnila N. Are we barking up the wrong vessels? Cerebral microcirculation after subarachnoid hemorrhage. Stroke. 2015;46(10):3014–9.
12. Ayer RE, Zhang JH. Oxidative stress in subarachnoid haemorrhage: significance in acute brain injury and vasospasm. Acta Neurochir Suppl. 2008;104:33–41.
13. Endo H, Nito C, Kamada H, Yu F, Chan PH. Reduction in oxidative stress by superoxide dismutase overexpression attenuates acute brain injury after subarachnoid hemorrhage via activation of Akt/glycogen synthase kinase-3beta survival signaling. J Cereb Blood Flow Metab. 2007;27(5):975–82.
14. Matz PG, Fujimura M, Lewen A, Morita-Fujimura Y, Chan PH. Increased cytochrome c-mediated DNA fragmentation and cell death in manganese-superoxide dismutase-deficient mice after exposure to subarachnoid hemolysate. Stroke. 2001;32(2):506–15.
15. Liu H, Zhao L, Yue L, Wang B, Li X, Guo H, et al. Pterostilbene attenuates early brain injury following subarachnoid hemorrhage via inhibition of the NLRP3 inflammasome and Nox2-related oxidative stress. Mol Neurobiol. 2017;54(8):5928–40.
16. Shi X, Fu Y, Zhang S, Ding H, Chen J. Baicalin attenuates subarachnoid hemorrhagic brain injury by modulating blood-brain barrier disruption, inflammation, and oxidative damage in mice. Oxidative Med Cell Longev. 2017;2017:1401790.
17. Zhan Y, Chen C, Suzuki H, Hu Q, Zhi X, Zhang JH. Hydrogen gas ameliorates oxidative stress in early brain injury after subarachnoid hemorrhage in rats. Crit Care Med. 2012;40(4):1291–6.
18. Park IS, Meno JR, Witt CE, Suttle TK, Chowdhary A, Nguyen TS, et al. Subarachnoid hemorrhage model in the rat: modification of the endovascular filament model. J Neurosci Methods. 2008;172(2):195–200.
19. Sugawara T, Ayer R, Jadhav V, Zhang JH. A new grading system evaluating bleeding scale in filament perforation subarachnoid hemorrhage rat model. J Neurosci Methods. 2008;167(2):327–34.
20. Garcia JH, Wagner S, Liu KF, Hu XJ. Neurological deficit and extent of neuronal necrosis attributable to middle cerebral artery occlusion in rats. Statistical validation. Stroke. 1995;26(4):627–34 discussion 635.
21. Wang L, Fumoto T, Masumoto S, Shoji T, Miura T, Naraoka M, et al. Regression of atherosclerosis with apple procyanidins by activating the ATP-binding cassette subfamily a member 1 in a rabbit model. Atherosclerosis. 2017;258:56–64.
22. Munakata A, Naraoka M, Katagai T, Shimamura N, Ohkuma H. Role of cyclooxygenase-2 in relation to nitric oxide and endothelin-1 on pathogenesis of cerebral vasospasm after subarachnoid hemorrhage in rabbit. Transl Stroke Res. 2016;7(3):220–7.
23. Chen J, Chen G, Li J, Qian C, Mo H, Gu C, et al. Melatonin attenuates inflammatory response-induced brain edema in early brain injury following a subarachnoid hemorrhage: a possible role for the regulation of pro-inflammatory cytokines. J Pineal Res. 2014;57(3):340–7.
24. Han Y, Zhang T, Su J, Zhao Y, Chenchen W, et al. Apigenin attenuates oxidative stress and neuronal apoptosis in early brain injury following subarachnoid hemorrhage. J Clin Neurosci. 2017;40:157–62.
25. Zhang ZY, Jiang M, Fang J, Yang MF, Zhang S, Yin YX, et al. Enhanced therapeutic potential of nano-curcumin against subarachnoid hemorrhage-induced blood-brain barrier disruption through inhibition of inflammatory response and oxidative stress. Mol Neurobiol. 2017;54(1):1–14.
26. Yabluchanskiy A, Ma Y, Iyer RP, Hall ME, Lindsey ML. Matrix metalloproteinase-9: many shades of function in cardiovascular disease. Physiology (Bethesda). 2013;28(6):391–403.
27. O'Sullivan S, Medina C, Ledwidge M, Radomski MW, Gilmer JF. Nitric oxide-matrix metaloproteinase-9 interactions: biological and pharmacological significance—NO and MMP-9 interactions. Biochim Biophys Acta. 2014;1843(3):603–17.
28. Duris K, Lipkova J, Splichal Z, Madaraszova T, Jurajda M. Early inflammatory response in the brain and anesthesia recovery time evaluation after experimental subarachnoid hemorrhage. Transl Stroke Res. 2018. https://doi.org/10.1007/s12975-018-0641-z.
29. Blecharz-Lang KG, Wagner J, Fries A, Nieminen-Kelhä M, Rösner J, Schneider UC, et al. Interleukin 6-mediated endothelial barrier disturbances can be attenuated by blockade of the IL6 receptor expressed in brain microvascular endothelial cells. Transl Stroke Res. 2018;9:631–42. https://doi.org/10.1007/s12975-018-0614-2.
30. Pang J, Chen Y, Kuai L, Yang P, Peng J, Wu Y, et al. Inhibition of blood-brain barrier disruption by an apolipoprotein E-mimetic peptide ameliorates early brain injury in experimental subarachnoid hemorrhage. Transl Stroke Res. 2017;8:257–72.
31. Zhang XS, Zhang X, Zhang QR, Wu Q, Li W, Jiang TW, et al. Astaxanthin reduces matrix metalloproteinase-9 expression and activity in the brain after experimental subarachnoid hemorrhage in rats. Brain Res. 2015;1624:113–24.
32. Zhang T, Su J, Guo B, Zhu T, Wang K, Li X. Ursolic acid alleviates early brain injury after experimental subarachnoid hemorrhage by

suppressing TLR4-mediated inflammatory pathway. Int Immunopharmacol. 2014;23(2):585–91.
33. Fujiwara N, Som AT, Pham LD, Lee BJ, Mandeville ET, Lo EH, et al. A free radical scavenger edaravone suppresses systemic inflammatory responses in a rat transient focal ischemia model. Neurosci Lett. 2016;633:7–13.
34. Yuan Y, Zha H, Rangarajan P, Ling EA, Wu C. Anti-inflammatory effects of edaravone and scutellarin in activated microglia in experimentally induced ischemia injury in rats and in BV-2 microglia. BMC Neurosci. 2014;15:125.
35. Yagi K, Kitazato KT, Uno M, Tada Y, Kinouchi T, Shimada K, et al. Edaravone, a free radical scavenger, inhibits MMP-9-related brain hemorrhage in rats treated with tissue plasminogen activator. Stroke. 2009;40(2):626–31.
36. Bache S, Rasmussen R, Rossing M, Laigaard FP, Nielsen FC, Møller K. MicroRNA changes in cerebrospinal fluid after subarachnoid hemorrhage. Stroke. 2017;48(9):2391–8.
37. Xu G, Meng L, Yauan D, Li K, Zhang Y, Dang C, et al. MEG3/miR-21 axis affects cell mobility by suppressing epithelial-mesenchymal transition in gastric cancer. Oncol Rep. 2018;40(1):39–48.
38. Zhou C, Ding J, Wu Y. Resveratrol induces apoptosis of bladder cancer cell via miR-21 regulation of Akt/Bcl-2 signaling pathway. Mol Med Rep. 2014;9(4):1467–73.
39. Obermeier B, Daneman R, Ransohoff RM. Development, maintenance and disruption of the blood-brain barrier. Nat Med. 2013;19(12):1584–96.
40. Tso MK, Macdonald RL. Subarachnoid hemorrhage: a review of experimental studies on the microcirculation and the neurovascular unit. Transl Stroke Res. 2014;5(2):174–89.
41. Friedrich B, Müller F, Feiler S, Schöller K, Plesnila N. Experimental subarachnoid hemorrhage causes early and long-lasting microarterial constriction and microthrombosis: an in-vivo microscopy study. J Cereb Blood Flow Metab. 2012;32(3):447–55.
42. Sehba FA, Friedrich V, Makonnen G, Bederson JB. Acute cerebral vascular injury after subarachnoid hemorrhage and its prevention by administration of a nitric oxide donor. J Neurosurg. 2007;106(2):321–9.
43. Ohkuma H, Itoh K, Shibata S, Suzuki S. Morphological changes of intraparenchymal arterioles after experimental subarachnoid hemorrhage in dogs. Neurosurgery. 1997;41(1):230–5 discussion 235-6.
44. Uhl E, Lehmberg J, Steiger HJ, Messmer K. Intraoperative detection of early microvasospasm in patients with subarachnoid hemorrhage by using orthogonal polarization spectral imaging. Neurosurgery. 2003;52(6):1307–15 discussion 1315-7.
45. Sun BL, Zheng CB, Yang MF, Yuan H, Zhang SM, Wang LX. Dynamic alterations of cerebral pial microcirculation during experimental subarachnoid hemorrhage. Cell Mol Neurobiol. 2009;29(2):235–41.
46. Liu H, Dienel A, Schöller K, Schwarzmaier SM, Nehrkorn K, Plesnila N, et al. Microvasospasms after experimental subarachnoid hemorrhage do not depend on endothelin a receptors. Stroke. 2018;49(3):693–9.
47. Sweeney MD, Ayyadurai S, Zlokovic BV. Pericytes of the neurovascular unit: key functions and signaling pathways. Nat Neurosci. 2016;19(6):771–83.
48. Peppiatt CM, Howarth C, Mobbs P, Attwell D. Bidirectional control of CNS capillary diameter by pericytes. Nature. 2006;443(7112):700–4.
49. Hall CN, Reynell C, Gesslein B, Hamilton NB, Mishra A, Sutherland BA, et al. Capillary pericytes regulate cerebral blood flow in health and disease. Nature. 2014;508(7494):55–60.
50. Yemisci M, Gursoy-Ozdemir Y, Vural A, Can A, Topalkara K, Dalkara T. Pericyte contraction induced by oxidative-nitrative stress impairs capillary reflow despite successful opening of an occluded cerebral artery. Nat Med. 2009;15(9):1031–7.
51. Zhang T, Su J, Wang K, Zhu T, Li X. Ursolic acid reduces oxidative stress to alleviate early brain injury following experimental subarachnoid hemorrhage. Neurosci Lett. 2014;579:12–7.
52. Zhang XS, Zhang X, Zhou ML, Zhou XM, Li N, Li W, et al. Amelioration of oxidative stress and protection against early brain injury by astaxanthin after experimental subarachnoid hemorrhage. J Neurosurg. 2014;121(1):42–5.
53. Guo D, Wilkinson DA, Thompson BG, Pandey AS, Keep RF, Xi G, et al. MRI characterization in the acute phase of experimental subarachnoid hemorrhage. Transl Stroke Res. 2017;8(3):234–43.
54. Sehba FA, Mostafa G, Friedrich V, Bederson JB. Acute microvascular platelet aggregation after subarachnoid hemorrhage. J Neurosurg. 2005;102(6):1094–100.
55. Suzuki S, Kimura M, Souma M, Ohkima H, Shimizu T, Iwabuchi T. Cerebral microthrombosis in symptomatic cerebral vasospasm—a quantitative histological study in autopsy cases. Neurol Med Chir (Tokyo). 1990;30(5):309–16.
56. Pisapia JM, Xu X, Kelly J, Yeung J, Carrion G, Tong H, et al. Microthrombosis after experimental subarachnoid hemorrhage: time course and effect of red blood cell-bound thrombin-activated pro-urokinase and clazosentan. Exp Neurol. 2012;233(1):357–63.
57. Muroi C, Fujioka M, Mishima K, Irie K, Fujimura Y, Nakano T, et al. Effect of ADAMTS-13 on cerebrovascular microthrombosis and neuronal injury after experimental subarachnoid hemorrhage. J Thromb Haemost. 2014;12(4):505–14.
58. Liu ZW, Gu H, Zhang BF, Zhao YH, Zhao JJ, Zhao YL, et al. Rapidly increased vasopressin promotes acute platelet aggregation and early brain injury after experimental subarachnoid hemorrhage in a rat model. Brain Res. 2016;1639:108–19.
59. Sabri M, Ai J, Knight B, Tariq A, Jeon H, Shang X, et al. Uncoupling of endothelial nitric oxide synthase after experimental subarachnoid hemorrhage. J Cereb Blood Flow Metab. 2011;31(1):190–9.
60. Sabri M, Ai J, Marsden PA, Macdonald RL. Simvastatin re-couples dysfunctional endothelial nitric oxide synthase in experimental subarachnoid hemorrhage. PLoS One. 2011;6(2):e17062.
61. Sabri M, Ai J, Lass E, D'abbondanza J, Macdonald RL. Genetic elimination of eNOS reduces secondary complications of experimental subarachnoid hemorrhage. J Cereb Blood Flow Metab. 2013;33(7):1008–14.